Evaluating the effects of drift angle on the self-propelled ship using Blade Element Momentum Theory

Yifu Zhang*, Dominic Hudson*, Björn Windén†, Stephen Turnock*
*Maritime Engineering Research Group, University of Southampton, UK
†SHORTCUt CFD LLC, College Station, Texas, USA
Corresponding email: yz26g15@soton.ac.uk

1 Introduction

Ship maneuverability is one of the most essential performance indicators in the ship design process. Common practice for predicting a ship's maneuvering characteristics and force derivatives includes theoretical methods, towing tank tests and numerical approaches via Computational Fluid Dynamics (CFD). Theoretical methods are mainly applicable to slender bodies and the interactions between the hull, the propeller and the rudder are usually not considered. In a towing tank test, forces and moments on the model ship can be measured in static and dynamic Planar Motion Mechanism (PMM) tests or Circular Motion Test (CMT) (Islam and Soares, 2018). However, conducting maneuvering tests in a towing tank or wave basin requires more accurate test facilities and ship models, which are very costly. Although traditional experimental tests in a conventional towing tank plays a significant role in evaluating ship's maneuvering performance, with rapid development in high performance computers and numerical techniques, CFD tools provides researchers with a more efficient and economic method to compute ship maneuvering characteristics on more complex and realistic ship geometries.

Carrica et al.(2013) conducted model and full-scale CFD computations of a surface combatant undergoing turning circle and zig-zag maneuvers using a simplified body force propeller model and adopted an overset grid approach to capture the ship motions and rudder movement. The URANS code CFDShip-Iowa was used for simulations and results agreed well with experimental data. Sigmund and el Moctar (2017) applied a sliding mesh approach to compute the complex hull-propeller-rudder interaction and predicted free running ship behavior in waves. This demonstrates the capability of numerical method in simulating ship maneuvering performance. More recently, Sanada et al. (2021) investigated the hull-propeller-rudder interactions of the KRISO Container Ship (KCS) with the aim of providing a physical explanation for the differences between the port and starboard turning circles using a combined experimental and CFD method. Although numerical methods can, in principle, provide an adequate description of all physics, this kind of analysis is still considered as state-of-art research rather than engineering practice (Zhang et al., 2017). On the one hand, large computational resources and long CPU time are required in numerical approaches. On the other hand, according to Skejic (2013), many technical difficulties concerning the analysis of ship maneuvering in realistic seaway are still not solved, such as the accuracy of the selected turbulence model, the adequacy of the propeller and rudder models under large angles of attack, the appearance of the crossflow shed vortices and more.

Therefore, this paper aims to study the self-propelled KCS at a series of fixed drift angles, which represent different stages of a maneuver. This is done instead of studying the complete time varying maneuver. This kind of modelling not only significantly reduces the computational cost but also helps to guide future experimental measurements of rudder and propeller forces. Detailed results and discussion on the influence of a series of drift angles on resistance, wake velocity contours, side force and yaw moment will be presented. All simulations are conducted in calm water condition using the open source RANS solver simpleFoam which is part of OpenFOAM v7.

2 Methodology

2.1Numerical model

The flow is modelled using the Reynolds Averaged Navier-Stokes equations. With the assumption of an incompressible fluid, the set of equations can be written in the form:

$$\frac{\partial \bar{U}_i}{\partial x_i} = 0 \tag{1}$$

$$\frac{\partial \overline{U_\iota}}{\partial \mathrm{t}} + \frac{\partial \overline{U_J U_\iota}}{\partial x_j} = -\frac{1}{\rho}\frac{\partial \overline{\mathrm{P}}}{\partial x_i} + \frac{\partial}{\partial x_j}\left(\nu\left(\frac{\partial \overline{U_\iota}}{\partial x_j} + \frac{\partial \overline{U_J}}{\partial x_i}\right)\right) - \frac{\partial \overline{u'_\iota u'_J}}{\partial x_j} + \overline{f_\iota} \quad (2)$$

Where x_i represents the Cartesian coordinates (X, Y, Z) and $\overline{U_\iota}$ are the Cartesian mean velocity components ($\overline{U_x}$, $\overline{U_y}$, $\overline{U_z}$). The Reynolds stress is expressed as ($\overline{u'_\iota u'_J}$) and must be modelled using an appropriate turbulence model. The SST k-ω turbulence model is adopted to achieve turbulence closure. The SST k-ω model has previously been successfully used for wakefield analysis and hull-propeller-rudder interaction (Larsson et al., 2015). Pressure-velocity coupling is obtained by using the SIMPLE algorithm. Only the underwater body of the KCS hull is included and a symmetry plane boundary condition is enforced at the still water plane to emulate a double model flow. Discretisation of the convection terms are achieved using a Gauss linear second order upwind scheme and the diffusion terms are resolved using the central difference scheme.

2.2Propeller model

To reduce the computational cost in the self-propelled calculations, propeller modelling using a body force model is used. This eliminates the need to mesh the propeller geometry. This means that the momentum generated by the rotating blades is directly inserted in the Navier-Stokes equation as an extra momentum source term or body force. Considering the momentum equation in Cartesian coordinates, the flow $\bar{u} = (u, v, w)$ is accelerated by the body force$\overline{F_{\bar{v}}} = (F_{vx}, F_{vy}, F_{vz})$. This force is only non-zero where the propeller is acting on the fluid.

$$\frac{\partial(\rho \mathrm{u})}{\partial \mathrm{t}} + \nabla \cdot (\rho u \bar{u}) = -\frac{\partial \mathrm{p}}{\partial \mathrm{x}} + \frac{\partial \tau_{xx}}{\partial \mathrm{x}} + \frac{\partial \tau_{yx}}{\partial \mathrm{y}} + \frac{\partial \tau_{zx}}{\partial \mathrm{z}} + \rho F_{vx} \quad (3)$$

$$\frac{\partial(\rho \mathrm{v})}{\partial \mathrm{t}} + \nabla \cdot (\rho v \bar{u}) = -\frac{\partial \mathrm{p}}{\partial \mathrm{y}} + \frac{\partial \tau_{xy}}{\partial \mathrm{x}} + \frac{\partial \tau_{yy}}{\partial \mathrm{y}} + \frac{\partial \tau_{zy}}{\partial \mathrm{z}} + \rho F_{vy} \quad (4)$$

$$\frac{\partial(\rho \mathrm{w})}{\partial \mathrm{t}} + \nabla \cdot (\rho w \bar{u}) = -\frac{\partial \mathrm{p}}{\partial \mathrm{z}} + \frac{\partial \tau_{xz}}{\partial \mathrm{x}} + \frac{\partial \tau_{yz}}{\partial \mathrm{y}} + \frac{\partial \tau_{zz}}{\partial \mathrm{z}} + \rho F_{vz} \quad (5)$$

There are various methods to compute the distribution of this force $\overline{F_{\bar{v}}}$, how it relates to the propeller geometry and how it is affected by the propeller inflow. A range of models with various levels of complexity exist; from a simple actuator disk where the force is spread over the radius according to an ideal distribution, to a full panel code for the propeller where the force is obtained from the pressure on each panel.

In this paper, Blade Element Momentum theory (BEMt) is used to model the propeller. Blade Element Momentum theory combines axial momentum theory and 2D blade element theory, which was first suggested by Burrill (1944). The theory is suitable for calculations on marine propellers close to the design working condition. It is based on the lift and drag generated by an airfoil with the angle of attack being determined by the local pitch and the incidence of the incoming velocity. This is obtained by the rotation of the propeller as well as the characteristics of the nominal wake (Windén, 2014). The coupling between blade element and momentum theory is achieved by equating their two estimates of efficiency. BEMt also requires the lift and drag properties of the blade section to be known *a priori*. Here,C_L is estimated from the force balance of thrust in the previous iteration and C_D is obtained by curve fitting to an experimentally measured $C_D - \alpha$ curve. The implementation of the BEMt in this paper follows the procedure by Molland et al. (2017). Such a coupling of RANS and BEMt has been successfully achieved in predicting ship hydrodynamic performance and hull-propeller-rudder interaction (Phillips et al., 2010; Windén, 2014; Badoe, 2015). Likewise, BEMt has been proved to be an accurate and cost-effective method for evaluation of maneuvering coefficients of a self-propelled ship (Phillips et al., 2009).

3 Computational implementations

The model ship used in this research for simulation is the KRISO Container Ship (KCS), which is a benchmark case for determining the flow around a modern container ship. Experimental data regarding

the self propulsion performance of the KCS was released as part of the Tokyo 2015 workshop on numerical hydrodynamics (Hino et al., 2020).

Table 1: Calculation conditions of KCS

Property	Model Scale	Full Scale
Lpp	7.2786m	230m
Fn(Lpp)	0.260 (2.196m/s)	0.260 (24kn)
Wetted surface area	9.4379 m^2	9424 m^2
Propeller		
Diameter	0.25m	7.9m
No. Blades	5	5
Rotation direction	Clockwise	Clockwise

Table 2: Total mesh sizes for cases with different drift angles

Drift Angle β(°)	Total Mesh Size
0	11.1M
5	13.8M
10	17.0M
15	20.3M
20	19.7M

The OpenFOAM utilities blockMesh and snappyHexMesh are used to generate the mesh. For each simulation, the first 1000 iterations are conducted as a bare hull resistance test using simpleFoam. Another 1000 iterations are then conducted as a self propulsion test, with BEMt propeller model, using the custom solver selfPropsimpleFoam, which is part of the SHORTCUt open source framework for ship performance analysis (Winden, 2021). Five cases are simulated in calm water condition, with drift angles of $\beta = 0°, 5°, 10°, 15°, 20°$ respectively. In all cases, Lpp is set to 1. Fig 1 shows the computational domain. The inlet is located 2.5Lpp from the bow; the outlet is 5Lpp from the stern; the side and the bottom are both 1.5Lpp from the hull surface.

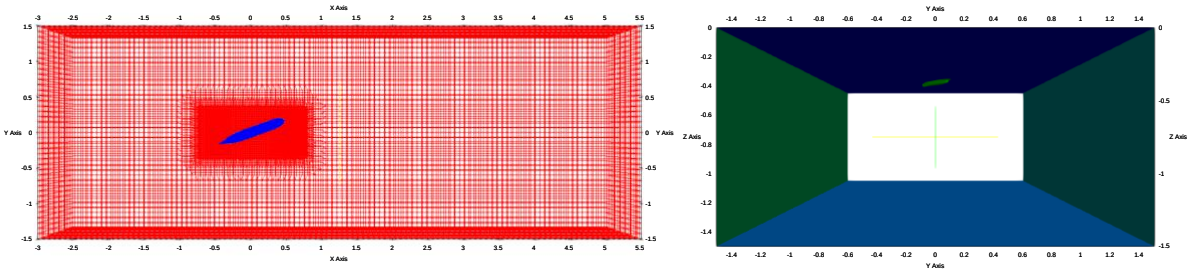

Fig. 1: Computational domain: top view and rear view

4 Results and discussion

4.1Resistance coefficients and side force, yaw moment

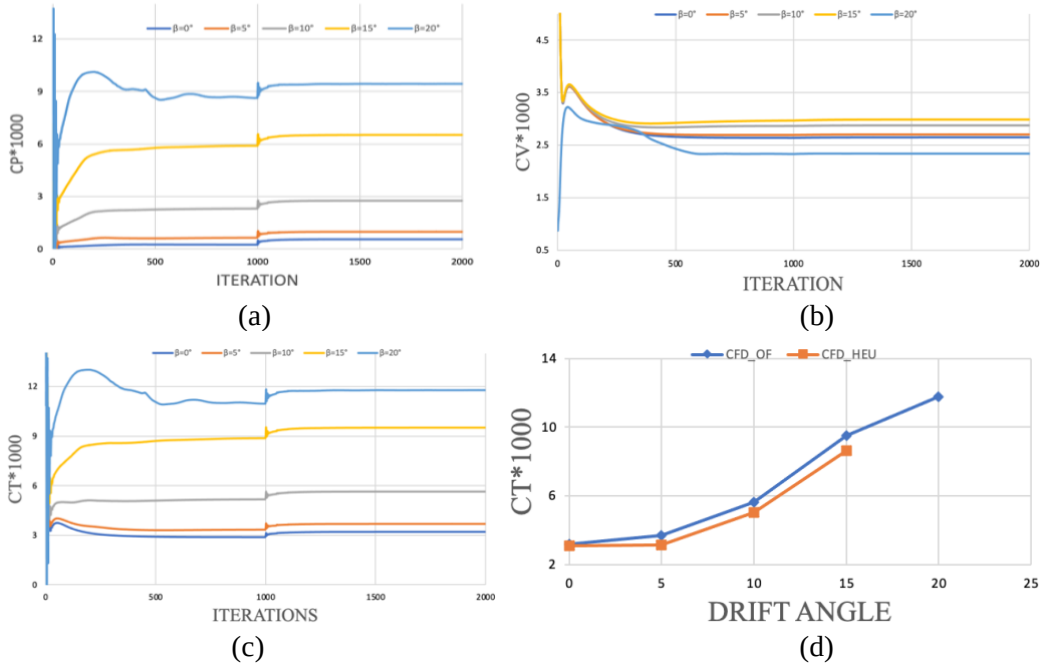

Fig 2: Resistance coefficients of KCS for different drift angles β.

As shown in Fig 2 (c), with the increase in static drift angle, the total resistance coefficient for the ship also increases. In terms of the viscous resistance component Fig 2 (b), it increases slightly with increasing drift angle ranging from 0° to 15°, and the value of viscous resistance coefficient is 0.00275. However, when the drift angle increases to 20°, the viscous resistance coefficient reduces to about 0.0024. The trend of pressure resistance and total resistance is very similar once the value of the viscous resistance converges after about 500 iterations. The addition of propeller forcing does not significantly change the value of the viscous resistance component. Experimental data for the drag force is not available, comparisons have been made with other simulation results seen in Fig 2 (d) (Sun et al., 2018), with which good agreement can be found. The difference is due to the fact that Sun et al. (2018) measured the different wetted surface areas for each drift angle while the constant experimental value of wetted surface is used in the current study.

Side force and yaw moment on the hull are calculated and both values are non-dimensionalised as shown below. To validate the accuracy of the results, two sets of experimental data and one set of numerical results are used, these are presented by Kim et al.(2015) and Islam and Guedes Soares (2018).

$$F'_Y = \frac{f_y(N)}{\rho \times U^2 \times L_{pp}^2} \; and \quad M'_Z = \frac{m_z}{\rho \times U^2 \times L_{pp}^3} \tag{6}$$

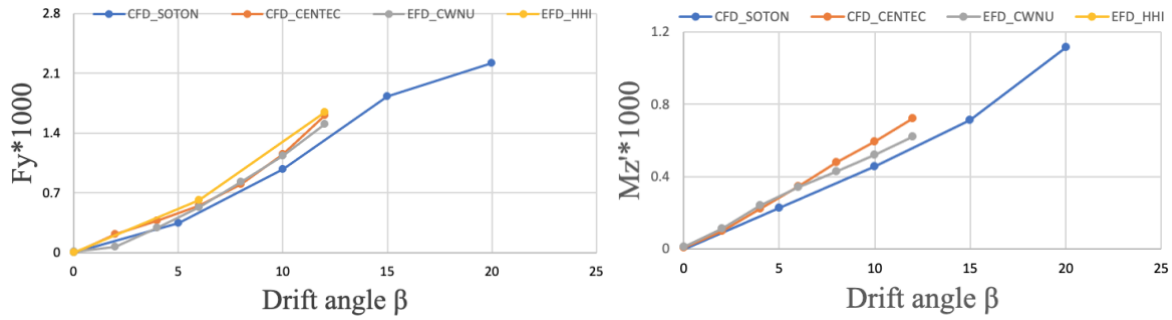

Fig 3: Non-dimensional sideforce and yaw moment experienced by KCS for different drift angles β

As shown in Fig 3, the simulations can capture the trend of side force and yaw moment. Two sets of experimental data display slight disagreement with each other, which could be due to different scales of the ship models and test facilities used. The current results, derived from OpenFOAM, show both a slightly lower side force and yaw moment compared to the other results. But the trend is similar, and deviation is less than 10%. The reason for that difference could be the absence of the free surface effect in current study. Overall, the simulations indicate that, with increasing static drift angle, the lateral force and yaw moment encountered by the KCS model increases.

4.2 Axial velocity contours and pressure distribution

The axial flow contour behind the propeller of the KCS was presented as part of the benchmarking data in the 2015 Tokyo workshop. This is compared with that calculated by the BEMt model below.

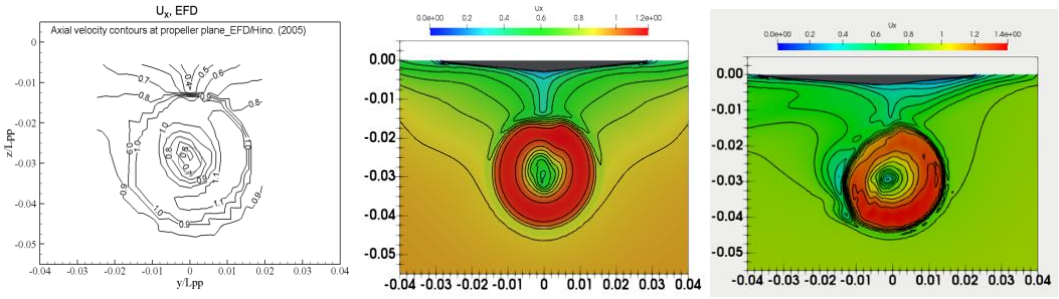

Fig 4: Local axial flow (Ux) at x/Lpp=0.4911. Middle: $\beta = 0°$, Right: $\beta = 10°$

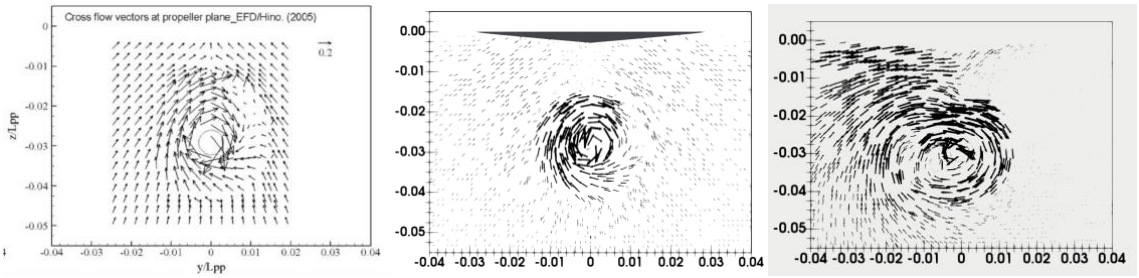

Fig 5: Cross flow vectors at x/Lpp=0.4911. Middle: $\beta = 0°$, Right: $\beta = 10°$

Because of the addition of the angular momentum term, the dominant velocity component can be seen at the left-hand side of the graph in both experimental and numerical results. When the drift angle of 10° is applied, the asymmetric wake profile is more evident. This indicates that results obtained from BEMt are quite promising.

Fig 6 shows the pressure distribution on the surface of the KCS bow at different drift angles. As can be seen, in drift motions, the maximum pressure peak is encountered by the front of the bow. With the increase in drift angle, pressure encountered by the KCS model also increases and the pressure peak shifts to the side.

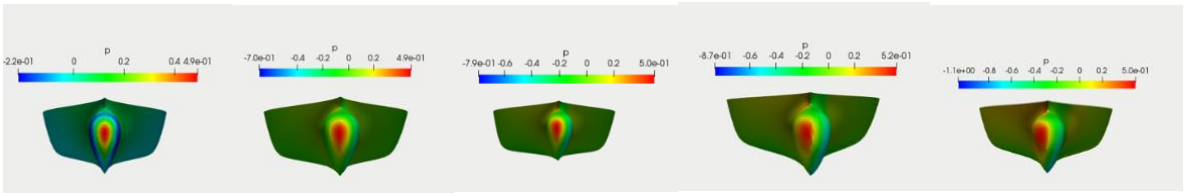

Fig 6: Hydrodynamic pressure distribution at bow of KCS at 0°,5°,10°,15°,20° drift angle.

4.3 Self-propulsion coefficients

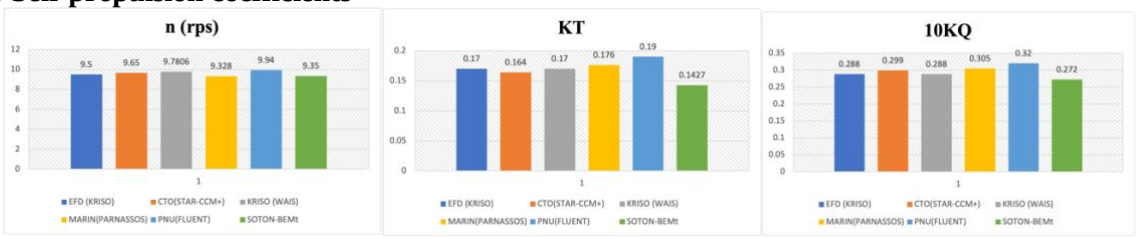

Fig 7: Comparison of estimated RPM for self propulsion and propulsion coefficients of KCS at β=0°.

There were only four submissions to the 2015 Tokyo workshop which presented results for a calculated self propulsion point of the KCS. The results in the current study are shown together with the submission that vary the RPM in Fig7. The results obtained by RANS-BEMt coupling method fares slightly less well against that of other institutions. This is likely due to the increased importance of the free surface effect for the KCS; in terms of the pressure distribution on the hull and the propeller. Fig 8 shows the variation of KT and 10KQ value with the increase of the drift angle.

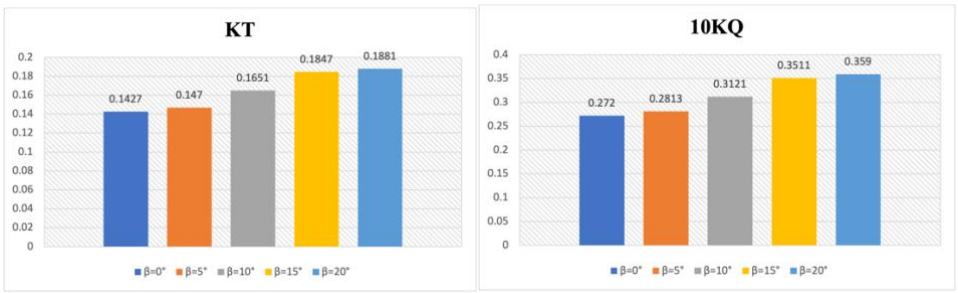

Fig 8: KT and 10KQ values for different drift angles.

5 Conclusion and future work

This paper presents simulations of the KCS model at different static drift angles in calm water. The results, including resistance, lateral force, yaw moment, axial velocity, pressure distribution and self-propulsion coefficients, show good agreement with experimental data. It is concluded that OpenFOAM is capable of performing maneuverability related calculations with reasonable accuracy and computational cost. The BEMt can capture the hydrodynamic performance of a ship in static drifting condition. Further investigations will include the simulation of a hull in different waves condition with drifting and the detailed influence of drift angle on hull-propeller-rudder interaction in real seaways.

References

Badoe, C.E., 2015. Design practice for the stern hull of a future twin-skeg ship using a high fidwlity numerical approach. University of Southampton. https://doi.org/10.1109/fie.2016.7757408

Burrill, L., 1944. Calculation of marine propeller performance characteristics. Trans. NECIES. 60.

Carrica, P.M., Ismail, F., Hyman, M., Bhushan, S., Stern, F., 2013. Turn and zigzag maneuvers of a surface combatant using a URANS approach with dynamic overset grids. J. Mar. Sci. Technol. 18. https://doi.org/10.1007/s00773-012-0196-8

Hino, T., Larsson, L., Stern, F., Visonneau, M., Hirata, N., Kim, J., 2020. Numerical Ship Hydrodynamics: An Assessment of the Tokyo 2015 Workshop. Springer.

Islam, H., Guedes Soares, C., 2018. Estimation of hydrodynamic derivatives of a container ship using PMM simulation in OpenFOAM. Ocean Eng. 164. https://doi.org/10.1016/j.oceaneng.2018.06.063

Islam, H., Soares, C.G., 2018. A CFD study of a ship moving with constant drift angle in calm water and waves, in: Progress in Maritime Technology and Engineering - Proceedings of the 4th International Conference on Maritime Technology and Engineering, MARTECH 2018. https://doi.org/10.1201/9780429505294-22

Kim, H., Akimoto, H., Islam, H., 2015. Estimation of the hydrodynamic derivatives by RaNS simulation of planar motion mechanism test. Ocean Eng. 108. https://doi.org/10.1016/j.oceaneng.2015.08.010

Larsson, L., Stern, F., Visonneau, M., Hino, T., Hirata, N., Kim, J., 2015. Proceedings, Tokyo 2015 Workshop on CFD in Ship Hydrodynamics, in: Tokyo CFD Workshop.

Molland, A.F., Turnock, S.R., Hudson, D.A., 2017. Ship resistance and propulsion, Marine Propellers and Propulsion. https://doi.org/10.1016/B978-075068150-6/50014-0

Phillips, A.B., Turnock, S.R., Furlong, M., 2010. Accurate capture of propeller-rudder interaction using a coupled blade element momentum-RANS approach. Sh. Technol. Res. 57. https://doi.org/10.1179/str.2010.57.2.005

Phillips, A.B., Turnock, S.R., Furlong, M., 2009. Evaluation of manoeuvring coefficients of a self-propelled ship using a blade element momentum propeller model coupled to a Reynolds averaged Navier Stokes flow solver. Ocean Eng. 36. https://doi.org/10.1016/j.oceaneng.2009.07.019

Sanada, Y., Park, S., Kim, D.H., Wang, Z., Stern, F., 2021. Experimental and CFD Study of KCS Hull-Propeller-Rudder Interaction for Steady Turning Circles 1–17.

Sigmund, S., el Moctar, O., 2017. Numerical and experimental investigation of propulsion in waves. Ocean Eng. 144. https://doi.org/10.1016/j.oceaneng.2017.08.016

Skejic, R., 2013. Ships Maneuvering Simulations in a Seaway - How close are we to reality ? Int. Work. Next Gener. Naut. Traffic Model. 91–101.

Sun, S., Li, L., Wang, C., Zhang, H., 2018. Numerical prediction analysis of propeller exciting force for hull–propeller–rudder system in oblique flow. Int. J. Nav. Archit. Ocean Eng. 10. https://doi.org/10.1016/j.ijnaoe.2017.03.005

Winden, B., 2021. An Open-Source Framework for Ship Performance CFD. https://doi.org/10.5957/tos-2021-22

Windén, B., 2014. Powering Performance of a Self Propelled Ship in Waves. University of Southampton.

Zhang, W., Zou, Z.J., Deng, D.H., 2017. A study on prediction of ship maneuvering in regular waves. Ocean Eng. 137. https://doi.org/10.1016/j.oceaneng.2017.03.046